

# Joint Motion Estimation and Autofocus in SAR Imaging

George Papanicolaou  
Stanford University

Challenges in SAR  
IPAM

February 9, 2012

This is joint work with Liliana Borcea and Thomas Callaghan

# Outline

## Phase-Space Approach to Motion Estimation and Autofocus

- Introduction and Model

- Motion Estimation

- Autofocus

## Motion Estimation and Imaging of Complex Scenes

- Separation of Moving and Stationary Target Data

- Numerical Simulations

## Optimization Methods in Motion Estimation

## Summary and Future Work

# Outline

## Phase-Space Approach to Motion Estimation and Autofocus

Introduction and Model

Motion Estimation

Autofocus

## Motion Estimation and Imaging of Complex Scenes

Separation of Moving and Stationary Target Data

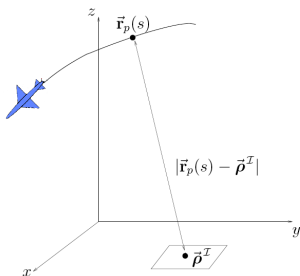
Numerical Simulations

## Optimization Methods in Motion Estimation

## Summary and Future Work

# Spotlight-mode Synthetic Aperture Radar (SAR) Imaging

Radar system emits probing signals  $f(t)$  and records echoes  $D(s, t)$  (slow time  $s$  of the SAR platform displacement, fast time  $t$  of the probing signal)



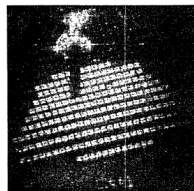
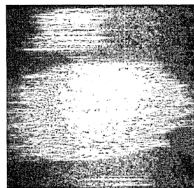
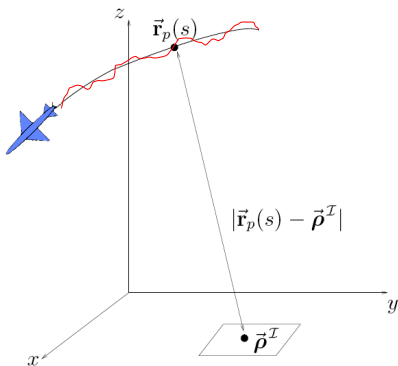
## X-band Regime

- ▶  $|\vec{r}_p(s) - \vec{\rho}^I| \approx 10 \text{ km}$
- ▶ Central wavelength  $\lambda_0 = 3\text{cm}$
- ▶ Bandwidth  $B=622 \text{ MHz}$
- ▶  $V = 70\text{m/s}$

$$\begin{aligned} \mathcal{I}(\vec{\rho}^I) &= \int_{-S(a)}^{S(a)} ds \int dt D(s, t) \overline{f(t - \tau(s, \vec{\rho}^I))} \\ &= \int_{\omega_0 - \pi B}^{\omega_0 + \pi B} \frac{d\omega}{2\pi} \int_{-S(a)}^{S(a)} ds \overline{\widehat{f}(\omega)} \widehat{D}(s, \omega) e^{-i\omega\tau(s, \vec{\rho}^I)} \end{aligned}$$

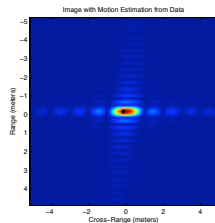
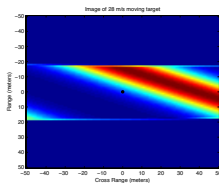
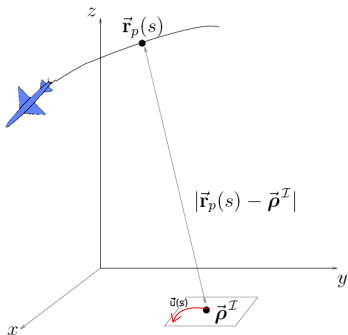
where  $\tau(s, \vec{\rho}^I) = 2|\vec{r}_p(s) - \vec{\rho}^I|/c$  is the roundtrip travel time

# Autofocus



- ▶ In practice, resolution always lost due to imperfect knowledge of the flight path
- ▶ Due to high frequency regime, a very small error in travel time can corrupt image
- ▶ Large bandwidth systems have potential for cm resolution but not without autofocus
- ▶ Previous Work:
  - ▶ Phase Gradient Autofocus (PGA): Jakowatz 1993
  - ▶ Contrast Metric Methods (Morrison 2007, etc)

# Motion Estimation



Similarly, motion of targets with sufficiently large reflectivity leads to poor image resolution

- ▶ Slow target motion yields similar results as platform perturbations
- ▶ Fast target motion smears image entirely

"Imaging Moving Targets from Scattered Waves", Cheney and Borden, IP 2008; Jen Jao  
 "Theory of SAR Imaging of a Moving Target", IEEE Trans Geosci and Rem Sens 2001.

# Phase-Space Methods

## Motivation for our approach

- ▶ High frequency regime results in highly oscillatory integrals
- ▶ In phase-space, small phase shifts can be determined robustly
- ▶ Use Wigner transform and ambiguity function because position of peaks relate to target motion and platform perturbations
- ▶ Use properly segmented “sub-apertures” of our data

Earlier work on phase space methods by Barbarosa (1992), Munson (2002) and others.

## Data Model

- ▶ Suppose a single point target  $\vec{\rho}(s)$  moves in imaging plane with velocity  $\vec{u}(s)$ 
  - ▶ Assume target location is known at some time  $s$
  - ▶ Assume velocity  $\vec{u}(s)$  is constant over small sub-aperture
- ▶ Suppose measured flight trajectory is  $\vec{r}_p(s)$  while actual trajectory is  $\vec{r}_p(s) + \vec{\mu}(s)$
- ▶ Assume single scattering (Born) approximation of solution to wave equation
- ▶ Regime: High frequency, relatively low bandwidth, long distance ( $\lambda_0 \ll L$ )
- ▶ Under these assumptions, the data model is:

$$D_r(s, t) = \frac{(\omega_o/c)^2}{(4\pi|\vec{r}_p(s) - \vec{\rho}(s)|)^2} f(t - (\tau(s, \vec{\rho}(s)) - \tau(s, \vec{\rho}_o))) \quad (1)$$

where we offset the travel time by a reference point  $\vec{\rho}_o$  in the imaging plane. The model of the range compressed data in the frequency domain is

$$\widehat{D}_r(s, \omega) \approx \frac{\omega_o^2}{c^2} \frac{|\widehat{f}_B(0)|^2 \mathbf{1}_{[\omega_o, \pi B]}(\omega)}{(4\pi|\vec{r}_p(s) - \vec{\rho}(s)|)^2} \exp \{i\omega [\tau(s, \vec{\rho}(s)) - \tau(s, \vec{\rho}_o)]\}. \quad (2)$$

where

$$\tau(s, \vec{\rho}(s)) = 2|\vec{r}_p(s) + \vec{\mu}(s) - \vec{\rho}(s)|/c$$



# Wigner Transform and Ambiguity Function of Data

- ▶ The Wigner transform of the data of a point target moving with velocity  $|\vec{\mathbf{u}}| \leq V$  is

$$\mathcal{W}(s, \Omega, \omega, T) = \int_{-\tilde{\Omega}}^{\tilde{\Omega}} d\tilde{\omega} \int_{-\tilde{S}}^{\tilde{S}} d\tilde{s} \hat{D}_r \left( s + \frac{\tilde{s}}{2}, \omega + \frac{\tilde{\omega}}{2} \right) \overline{\hat{D}_r \left( s - \frac{\tilde{s}}{2}, \omega - \frac{\tilde{\omega}}{2} \right)} e^{i\tilde{s}\Omega - i\tilde{\omega}T}$$

where  $\tilde{\Omega} = 2\pi B - 2|\omega - \omega_o|$  and  $\tilde{S} = \frac{a}{2V}$ .

- ▶ The ambiguity function of the data is

$$\mathcal{A}(s, \Omega, \tilde{s}, T) = \int_{\omega_o - \pi B}^{\omega_o + \pi B} d\omega \int_{-\bar{S}}^{\bar{S}} d\bar{s} \hat{D}_r \left( s + \bar{s} + \frac{\tilde{s}}{2}, \omega \right) \overline{\hat{D}_r \left( s + \bar{s} - \frac{\tilde{s}}{2}, \omega \right)} e^{i\bar{s}\Omega - i\omega T}$$

where  $\bar{S} = \frac{a}{2V}$ .

## Choice of these phase-space methods

- ▶ Wigner transform
  - ▶ Windowed Fourier Transform of offset in data
- ▶ Ambiguity function
  - ▶ Windowed cross-correlation transform
- ▶ Both transform two dimensional functions to four dimensional functions. However, we choose  $\omega$  and  $\tilde{s}$  to maximize the windowing, so result is two dimensional function for each time  $s$
- ▶ For small enough sub-apertures, both are products of sinc functions

# Phase-Space Transforms for Motion Estimation ( $\vec{\mu}(s) \equiv 0$ )

**Result<sup>1</sup>:** Under conditions on the size of the aperture that restrict the size of the Fresnel number  $a^2/(\lambda_0 L)$  so we can linearize phases

$$\mathcal{W}(s, \Omega, \omega_o, T) \sim \text{sinc}\{\pi B [T - \Delta\tau(s)]\} \text{sinc}\left\{\frac{4\pi a}{\lambda_o} \left[\frac{\Omega c}{2\omega_o V} - \Phi(s)\right]\right\}$$

$$\mathcal{A}\left(s, \Omega, \frac{a}{2V}, T\right) \sim \text{sinc}\left\{\frac{\pi B a}{c} \left[\frac{cT}{a} + \Phi(s)\right]\right\} \text{sinc}\left[\frac{a\Omega}{2V} + \frac{\pi a^2 \Phi^\perp(s)}{\lambda_o |\vec{r}_\rho(s) - \vec{\rho}(s)|}\right],$$

where  $\vec{m}(s)$  and  $\vec{t}(s)$  are the unit vectors

$$\vec{m}(s) = \frac{\vec{r}_\rho(s) - \vec{\rho}}{|\vec{r}_\rho(s) - \vec{\rho}|}, \quad \vec{t}(s) = \frac{\vec{r}'_\rho(s)}{V}$$

and  $\mathbb{P}(s) = I - \vec{m}(s)\vec{m}(s)^T$  is the projection matrix orthogonal to  $\vec{m}(s)$

$$\Delta\tau(s) = \tau(s, \vec{\rho}(s)) - \tau(s, \vec{\rho}_o) \quad \text{and} \quad \Phi(s) = \frac{\vec{u}}{V} \cdot \vec{m}(s) - \vec{t}(s) \cdot (\vec{m}(s) - \vec{m}_o(s)).$$

$$\Phi^\perp(s) = \left| \mathbb{P}(s) \left( \vec{t}(s) - \frac{\vec{u}}{V} \right) \right|^2 - |\vec{r}_\rho(s) - \vec{\rho}(s)| \left[ \frac{|\mathbb{P}_o(s)\vec{t}(s)|^2}{|\vec{r}_\rho(s) - \vec{\rho}_o|} - \frac{\vec{t}'(s)}{V} \cdot (\vec{m}(s) - \vec{m}_o(s)) \right],$$

<sup>1</sup>L. Borcea, T. Callaghan, G. Papanicolaou, *Synthetic Aperture Radar Imaging with Motion Estimation and Autofocus*, To appear in *Inverse Problems*.

# Complementary Phase Information for Motion Estimation

## Wigner Transform

- By selecting the peaks in the Wigner transform ( $\Omega^{\mathcal{W}}(s), T^{\mathcal{W}}(s)$ ) we can extract the estimate:

$$\frac{\vec{u}}{V} \cdot \vec{m}(s) = \frac{c \Omega^{\mathcal{W}}(s)}{2\omega_o V} + \vec{t}(s) \cdot \vec{m}(s) + O\left(\frac{\lambda_o}{a}\right)$$

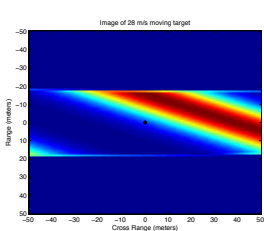
- Orthogonal estimate can be derived from peaks of Wigner transform, but requires a numerical differentiation

## Ambiguity Function

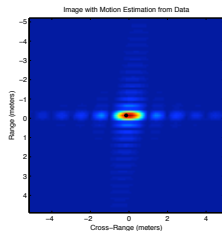
- By selecting the peaks in the ambiguity function ( $\Omega^{\mathcal{A}}(s), T^{\mathcal{A}}(s)$ ) we can extract an estimate of the velocity in an orthogonal direction  $|\mathbb{P}(s) (\vec{t}(s) - \frac{\vec{u}}{V})|^2$  and of  $\frac{\vec{u}}{V} \cdot \vec{m}(s)$  but with worse resolution than Wigner estimate.

The Wigner transform estimate of  $\frac{\vec{u}}{V} \cdot \vec{m}(s)$  and the ambiguity function estimate of  $|\mathbb{P}(s) (\vec{t}(s) - \frac{\vec{u}}{V})|^2$  are complementary estimates that can be combined to form an estimate of  $\vec{u}(s)$ .

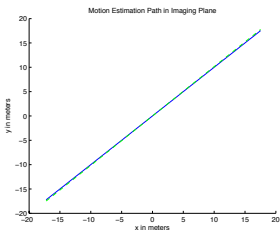
# Motion Estimation on Single Subaperture of Single Target



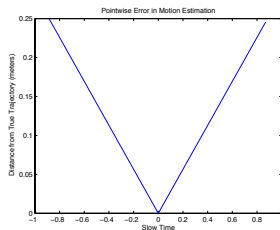
(a) Uncorrectd Image



(b) Correctd Image



(c) Estimated Motion



(d) Error

# Autofocus

$$\mathcal{I}(\rho^{\mathcal{I}}) = \int_{-S}^S ds \int_{\omega_o - \pi B}^{\omega_o + \pi B} \frac{d\omega}{2\pi} \widehat{D}_r(s, \omega) e^{-\frac{2i\omega}{c} (|\vec{r}_p(s) - \vec{\rho}^{\mathcal{I}}| - |\vec{r}_p(s) - \vec{\rho}_o|)}$$

Through similar approximation of phases by a second degree polynomial in  $s$  and the same constraints as before:

$$\begin{aligned} \mathcal{I}(\rho^{\mathcal{I}}) \sim \int_{\omega_o - \pi B}^{\omega_o + \pi B} d\omega \exp \left\{ \frac{2i\omega}{c} (|\vec{r}_p - \vec{\rho}| - |\vec{r}_p - \vec{\rho}^{\mathcal{I}}| + \varphi_0) \right\} \int_{-S}^S ds \exp \left\{ \frac{2i\omega s V}{c} [\vec{t} \cdot (\vec{m} - \vec{m}_{\mathcal{I}}) + \varphi_1] \right. \\ \left. + \frac{i\omega_o (sV)^2}{c} \left[ \frac{\vec{t}'}{V} \cdot (\vec{m} - \vec{m}_{\mathcal{I}}) + \frac{|\mathbb{P}\vec{t}|^2}{|\vec{r}_p - \vec{\rho}|} - \frac{|\mathbb{P}_{\mathcal{I}}\vec{t}|^2}{|\vec{r}_p - \vec{\rho}_*^{\mathcal{I}}|} + \varphi_2 \right] \right\}, \end{aligned}$$

The focusing of  $\mathcal{I}(\rho^{\mathcal{I}})$  is determined by the phases

$$\varphi_0 = \vec{m} \cdot \vec{\mu}, \quad \varphi_1 = \vec{m} \cdot \frac{\vec{\mu}'}{V} + \vec{t} \cdot \frac{\mathbb{P}\vec{\mu}}{|\vec{r}_p - \vec{\rho}|}, \quad \varphi_2 = \vec{m} \cdot \frac{\vec{\mu}''}{V^2} + \frac{2(\vec{t} + \frac{\vec{\mu}'}{V})}{|\vec{r}_p - \vec{\rho}|} \cdot \frac{\mathbb{P}\vec{\mu}'}{V}.$$

Autofocus process consists in applying the correction  $\vec{\mu}^{AF}(s) = \left[ \varphi_0 + sV \varphi_1 + \frac{(sV)^2}{2} \varphi_2 \right] \vec{m}$  to the SAR platform trajectory and forming the image

$$\mathcal{I}^{AF}(\rho^{\mathcal{I}}) = \int_{-S}^S ds \int_{\omega_o - \pi B}^{\omega_o + \pi B} \frac{d\omega}{2\pi} \widehat{D}_r(s, \omega) e^{-\frac{2i\omega}{c} (|\vec{r}_p(s) + \vec{\mu}^{AF}(s) - \vec{\rho}^{\mathcal{I}}| - |\vec{r}_p(s) - \vec{\rho}_o|)}.$$

# Phase-Space Transforms for Autofocus ( $\vec{u}(s) \equiv 0$ )

**Result:** Under conditions on the size of the aperture that restrict the size of the Fresnel number  $a^2/(\lambda_0 L)$

$$\mathcal{W}(s=0, \Omega, \omega_o, T) \sim \text{sinc} \left\{ \pi B \left[ T + \delta T^{\mathcal{W}} \right] \right\} \text{sinc} \left\{ \frac{4\pi a c (\Omega + \delta \Omega^{\mathcal{W}})}{2\lambda_o V \omega_o} \right\}$$

$$\mathcal{A} \left( s=0, \Omega, \frac{a}{2V}, T \right) \sim \text{sinc} \left\{ \pi B (T + \delta T^{\mathcal{A}}) \right\} \text{sinc} \left[ \frac{a(\Omega + \delta \Omega^{\mathcal{A}})}{2V} \right]$$

where

$$\delta T^{\mathcal{W}} = \frac{2\vec{\mu} \cdot \vec{m}}{c}, \quad \frac{c\delta \Omega^{\mathcal{W}}}{2V\omega_o} = \vec{m} \cdot \frac{\vec{\mu}'}{V} + \vec{t} \cdot \frac{\mathbb{P}\vec{\mu}}{|\vec{r}_p - \vec{\rho}|}.$$

and

$$\delta T^{\mathcal{A}} = -\frac{a}{V} \frac{\delta \Omega^{\mathcal{W}}}{\omega_o} \quad \text{and} \quad \frac{\delta \Omega^{\mathcal{A}}}{\omega_o} = \frac{Va}{c} \left[ \frac{2 \left( \vec{t} - \frac{\vec{u}}{V} \right)}{|\vec{r}_p - \vec{\rho}|} \cdot \frac{\mathbb{P}\vec{\mu}'}{V} + \frac{\vec{\mu}''}{V^2} \cdot \vec{m} \right].$$

# Complementary Phase Information for Autofocus

## Wigner Transform

- By selecting the peaks in the Wigner transform  $(\Omega^W(s), T^W(s))$  we can extract the estimate:

$$\varphi_0(s) = -\frac{c}{2} T^W(s) + O\left(\frac{c}{B}\right), \quad \varphi_1(s) = -\frac{\lambda_o}{4\pi V} \Omega^W(s) + O\left(\frac{\lambda_o}{a}\right).$$

## Ambiguity Function

- By selecting the peaks in the ambiguity function  $(\Omega^A(s), T^A(s))$  we can extract the estimate:

$$\varphi_1(s) = \frac{c}{2a} T^A(s) + O\left(\frac{c}{aB}\right), \quad \varphi_2(s) = -\frac{\lambda_o}{2\pi aV} \Omega^A(s) + O\left(\frac{\lambda_o}{a^2}\right).$$

Similarly, we get a redundant estimate of  $\varphi_1$ , with worse resolution, because

$$\frac{c}{aB} \sim \frac{\lambda_o}{a} \frac{\omega_o}{B} \gg \frac{\lambda_o}{a}.$$

The ambiguity function is useful for the estimation of  $\varphi_2$ , and thus complements the Wigner transform in the autofocus process.

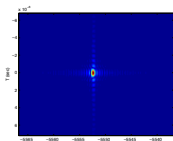


## Extending Single Scatterer Model

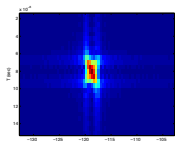
We can extend this approach to situations where the data consists of

- ▶ **Motion Estimation:** Cluster of targets moving together
- ▶ **Autofocus:** Cluster of stationary targets

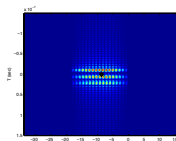
by computing the centroid of Wigner transform and ambiguity function instead of picking the peak



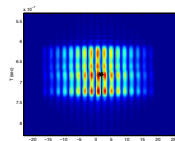
(a)  $W(\Omega, T)$  1 scatt



(b)  $A(\Omega, T)$  1 scatt



(c)  $W(\Omega, T)$  81 scatts

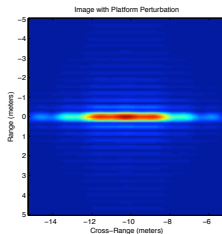


(d)  $A(\Omega, T)$  81 scatts

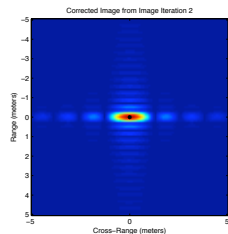
But what about more general scenes with several stationary targets and possibly multiple targets moving in different directions that you wish to track?

# Autofocus for a Single Scatterer Image

- ▶ Single Sub-Aperture  
( 100 m, 1 degree)

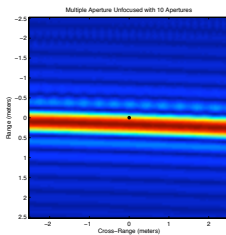


(a) Unfocused

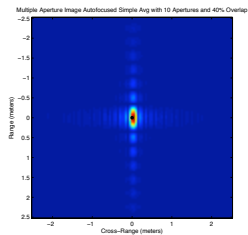


(b) Autofocused

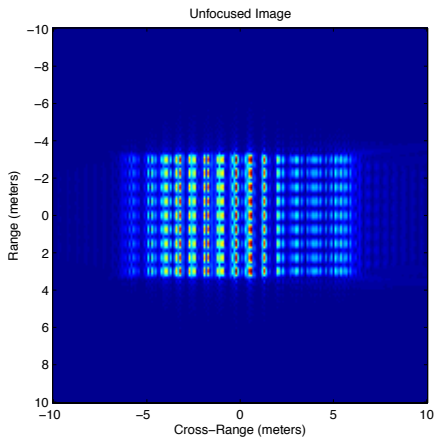
- ▶ 1 km Aperture (10 degrees)



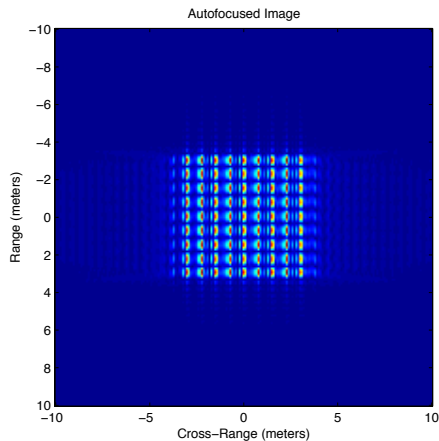
(c) Unfocused



(d) Autofocused

Autofocus over 1 km aperture ( $10^\circ$ ) with Complex Scene

(a) Unfocused



(b) Autofocused

# Outline

## Phase-Space Approach to Motion Estimation and Autofocus

- Introduction and Model

- Motion Estimation

- Autofocus

## Motion Estimation and Imaging of Complex Scenes

- Separation of Moving and Stationary Target Data

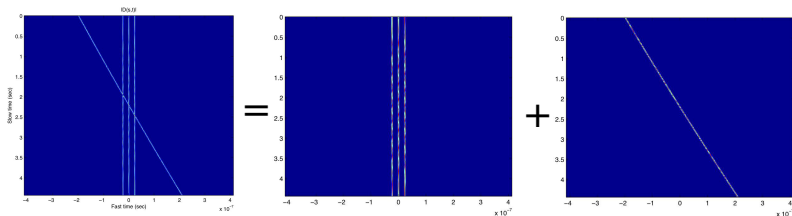
- Numerical Simulations

## Optimization Methods in Motion Estimation

## Summary and Future Work

# Can we separate stationary target data from moving target data?

Phase-space method works autofocus for stationary targets and motion estimation where all targets move with same velocity. In general we have more complex scenes. Ideally, we could decompose the data into stationary plus moving.



This motivates using a data pre-processing step to separate data:

- ▶ Robust PCA: Low Rank + Sparse Decomposition
- ▶ Geometric travel-time transformation and data filtering

After separation, we can apply existing algorithms individually for motion estimation and autofocus.

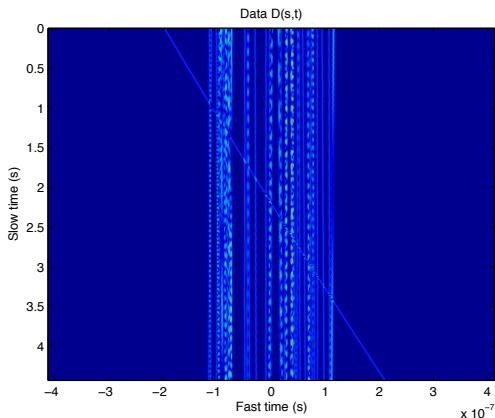
## Multiple Scatterer Model

Assuming Born (single scattering) approximation, we get superposition of traces

$$D_r(s, t) = \sum_{m=1}^M R_m f(t - (\tau(s, \vec{\rho}_m(s)) - \tau(s, \vec{\rho}_o))) + \sum_{n=1}^N R_n f(t - (\tau(s, \vec{\rho}_n) - \tau(s, \vec{\rho}_o)))$$

where  $\vec{\rho}_m(s)$  and  $\vec{\rho}_n$  denote the  $m$ -th moving target and the  $n$ -th stationary target respectively.  $R_m, R_n$  absorb the reflectivity and other amplitude terms.

$D_r(s, t)$  for sample scene



# Robust Principle Component Analysis (RPCA)

**Goal:** Decompose  $D(s, t) = D^n(s, t) + D^m(s, t) =$  stationary data + moving data.

**Idea:** Think of  $D(s, t)$  as a matrix  $M$ . Decompose into low rank  $L$  plus sparse  $S$

- ▶ Traces from stationary targets  $\approx$  columns in  $M$ .  
Structure  $\approx$  low rank part  $L$  of  $M$ .
- ▶ The remainder,  $S = M - L \approx$  trace from moving target.  
Structure  $\approx$  full rank, but sparse.

The RPCA method<sup>2</sup> does such decompositions of matrices, into a low rank part  $L$  and a sparse part  $S$ , by solving the following convex optimization problem:

$$\begin{aligned} & \text{minimize} && \|L\|_* + \lambda \|S\|_1 \\ & \text{subject to} && L + S = M. \end{aligned}$$

Here  $\|\cdot\|_*$  is the nuclear norm, i.e. the sum of the singular values, and  $\|\cdot\|_1$  is the matrix 1-norm. The Lagrange multiplier  $\lambda$  has the optimal value of  $1/\sqrt{\dim(M)}$ .

---

<sup>2</sup>Candes, E.J. and Li, X. and Ma, Y. and Wright, J., *Robust principal component analysis?*, Journal of ACM 58(1), 1-37, 2009

## RPCA Separation: 3 scatterers

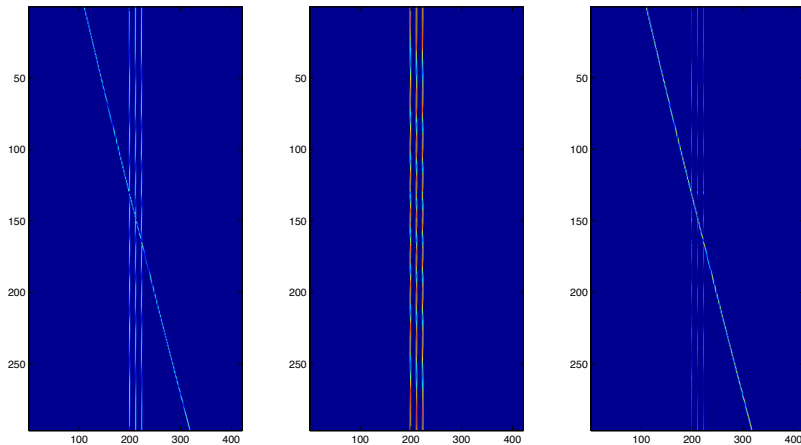


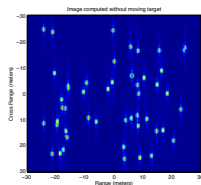
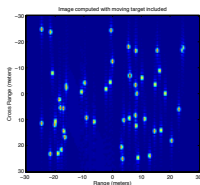
Figure:  $D_r(s, t) = L + S$  from RPCA. Fails to work because stationary targets are not low rank in this domain due to high frequency and hyperbolic responses.



# Geometric travel-time transformation and data filtering

**Idea:** Since the stationary targets can be imaged reasonably well, even in the presence of the platform trajectory perturbations, we can use the preliminary images in our data processing step.

1. Estimate locations of stationary targets from preliminary image  $\{\widehat{\vec{\rho}}_\ell\}$



2. Apply a geometrical transformation to  $D(s, t)$ , using travel times from the estimated platform location to one target at a time in the image,

$$\begin{aligned}
 D^{\widehat{\vec{\rho}}_\ell}(s, t) &= D_r \left( s, t + \left( \tau(s, \widehat{\vec{\rho}}_\ell) - \tau(s, \vec{\rho}_o) \right) \right) \\
 &= \sum_{m=1}^M f(t - (\tau(s, \vec{\rho}_m(s)) - \tau(s, \widehat{\vec{\rho}}_\ell))) + \sum_{n \neq \ell}^N f(t - (\tau(s, \vec{\rho}_n) - \tau(s, \widehat{\vec{\rho}}_\ell))) \\
 &\quad + f \left( t - \tau(s, \vec{\rho}_\ell) - \tau(s, \widehat{\vec{\rho}}_\ell) \right)
 \end{aligned}$$

When  $\widehat{\vec{\rho}}_\ell = \vec{\rho}_\ell$ , this transformation removes the slow time dependence of the trace of the echo from that particular target.

# Geometric travel-time transformation and data filtering

3. Remove this trace from the rest of the data using a filter. One technique, which has been successful in seismic imaging<sup>3</sup>, amounts in this case to taking an approximation to the derivative in slow time of the transformed data

$$[QD\widehat{P}_\ell](s, t) = D\widehat{P}_\ell(s, t) - \frac{1}{|I(h)|} \int_{I(h)} D\widehat{P}_\ell(s + h, t) dh$$

where  $I(h)$  is a small interval of length  $|I(h)|$ .

4. Repeat for each estimated stationary target location

---

<sup>3</sup>Borcea, L., Gonzalez del Cueto, F., Papanicolaou, G., Tsogka, C., *Filtering deterministic layering effects in imaging* SIAM Multiscale Model. Simul., Vol 7, No 3, 2009, pp. 1267-1301.

# Geometric travel-time transformation and data filtering

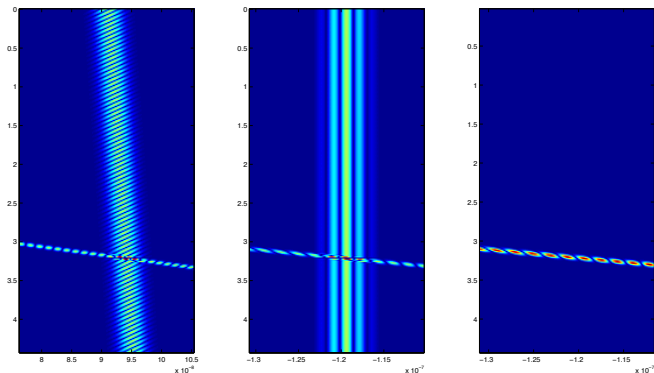


**Figure:** Filtering of a stationary scatterer. Left: Original trace. Middle: Transformed trace. Right: Filtered trace by slow time derivative. Notice that the stationary trace has been eliminated while the moving target trace remains.

# Travel-time transformation and Filtering Separation

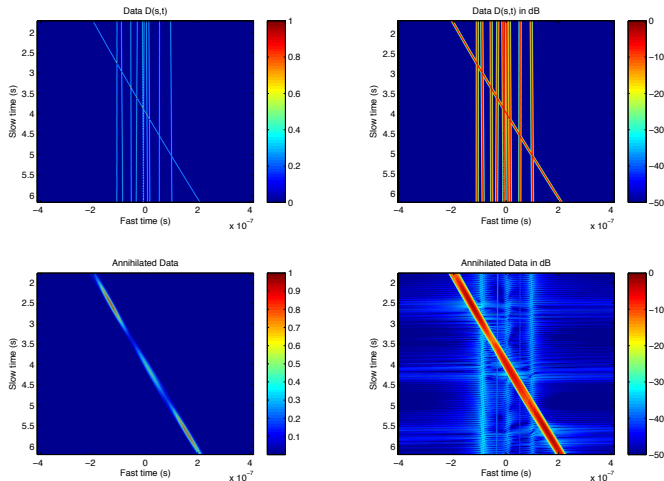
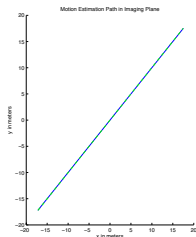
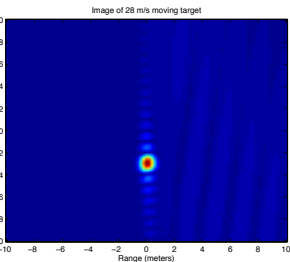
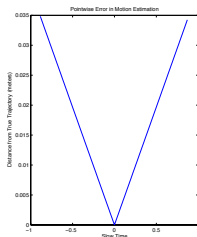


Figure: Before and after filtering of the data from a 10 stationary scatterer scene with a single moving target with velocity 28 m/s. Top/Bottom=Before/After. Right column is in dB scale

# Motion Estimation and Imaging



(a) Motion Estimate



(b) Moving Target Image

**Figure:** Motion estimation results for scene with 10 stationary scatterers and 1 moving target after annihilation. Left is the path and error. Right is the image of the moving target computed with estimated motion. It is displaced from  $(0, 0)$  because of small error in velocity estimation.

# Challenges

1. Inaccurate location estimates of stationary scatterers. Sensitivity analysis for this is work in progress.
2. Numerous applications of filter for scenes with numerous strong stationary scatterers degrade moving target signal. This is due to numerical differentiation of a function with limited sampling in slow time.
3. Slow moving targets

# Outline

## Phase-Space Approach to Motion Estimation and Autofocus

- Introduction and Model

- Motion Estimation

- Autofocus

## Motion Estimation and Imaging of Complex Scenes

- Separation of Moving and Stationary Target Data

- Numerical Simulations

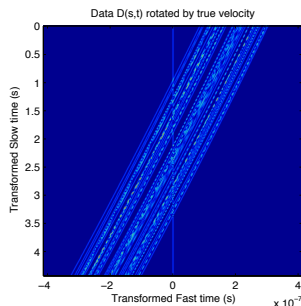
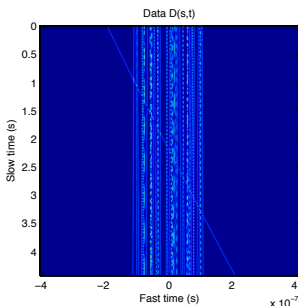
## Optimization Methods in Motion Estimation

## Summary and Future Work

# Velocity Search Optimization

Phase-space velocity estimation method struggles with too many stationary targets and multiple moving targets. Another approach to finding the velocity of the moving target is to search for the velocity  $\vec{u}^l$  that will correspond to “rotating and straightening” the traces so that those from the moving target become essentially independent of the slow time  $s$ .

$$D_r^{\vec{u}^l}(s, t) = D_r \left( s, t + \left( \tau(s, \vec{\rho}^l) - \tau(s, \vec{\rho}_o) \right) \right), \quad \tau(s, \vec{\rho}^l) = \frac{2}{c} (|\vec{r}_p(s) - (\vec{\rho}_o + \vec{u}^l s)|)$$





# Velocity Search Optimization

To motivate the choice of objective functions, we can model the phase of the pulse compressed data from a single moving target  $\vec{\rho}(s)$  as  $\widehat{D}\vec{\rho}(0)(s, \omega) \sim e^{\frac{2i\omega}{c}\phi(s)}$  where

$$\phi(s) = s (\mathbf{V}\vec{\mathbf{t}}(0) - \vec{\mathbf{u}}) \cdot \vec{\mathbf{m}}(0) + \frac{s^2 V^2}{2} \left( \frac{|\mathbb{P}(0) \left( \vec{\mathbf{t}}(0) - \frac{\vec{\mathbf{u}}}{V} \right)|^2}{|\vec{\mathbf{r}}_p(0) - \vec{\rho}(0)|} - \frac{\vec{\mathbf{n}}(0) \cdot \vec{\mathbf{m}}(0)}{R} \right)$$

Note that by choosing to transform the data with respect to  $\vec{\rho}(0)$ , we remove the travel time dependence.

Thus  $\vec{\mathbf{u}} \cdot \vec{\mathbf{m}}(0)$  affects the slope and  $\vec{\mathbf{u}} \cdot \vec{\mathbf{t}}(0)$  affects the curvature of the echoes.

- ▶ Motion in the direction of  $\vec{\mathbf{m}}_o$  has a stronger effect, so instead of searching for both components of  $\vec{\mathbf{u}}^l = (u_x^l, u_y^l)$ , we search first for  $\vec{\mathbf{u}}^l$  in the direction of  $\vec{\mathbf{m}}_o$ , the projection of  $\vec{\mathbf{m}}_o$  on the  $x - y$  plane.
- ▶ Search for component of the velocity in the direction  $\vec{\mathbf{t}}_o$ , where  $\vec{\mathbf{t}}_o$  is the unit vector tangent to the platform trajectory at the center of the aperture, and in the flight plane.

## Objective functions

1. Apply filter to suppress the stationary targets.
2. Search for  $\nu^* = \arg \max_{\nu} f(\nu; \vec{\mathbf{m}}_o)$  where

$$f(\nu; \vec{\mathbf{m}}_o) = \left\| \sum_s |[QD]^{\nu \mathbf{m}_o}(s, t)| \right\|_p$$

for some  $p$  norm for  $p \geq 2$ . Finds the velocity that “straightens” the moving target trace.

3. Search for  $\xi^* = \arg \min_{\xi} g(\xi; \vec{\mathbf{t}}_o, \nu^*)$  where

$$g(\xi; \vec{\mathbf{t}}_o, \nu^*) = \sum_{s,t} \left| [Q^2 [QD]^{\nu^* \mathbf{m}_o + \xi \mathbf{t}_o}](s, t) \right|$$

where  $Q^2$  denotes applying the annihilation filter twice. This approximates the second derivative in slow-time which should be zero when curvature is removed. The 1-norm is used to mitigate the effects of the imperfectly filtered stationary targets.

## Results

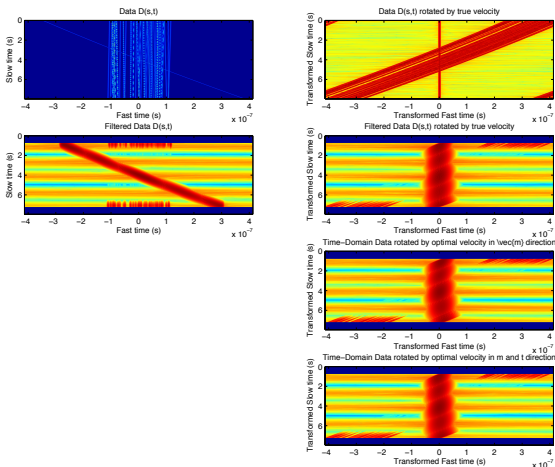
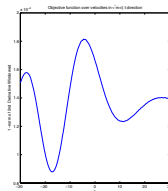
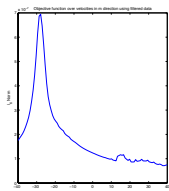
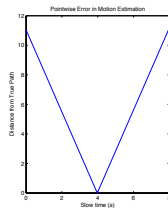
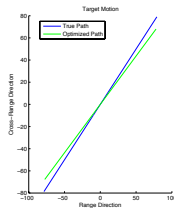


**Figure:** 50 stationary scatterer image with one moving target at 28 m/s. Comparison of data, data rotated by true velocity, filtered data, filtered data rotated by true velocity, filtered data rotated by optimal velocity in  $\vec{m}_o$  direction, and filtered data rotated by optimal velocity.

## Results



(a) Objective functions



(b) Velocity Estimation

Figure: Left objective function  $f(\nu; \vec{m}_o)$  and  $g(\xi; \vec{t}_o, \nu^*)$ . Right: estimated target path and error.

# Outline

## Phase-Space Approach to Motion Estimation and Autofocus

- Introduction and Model

- Motion Estimation

- Autofocus

## Motion Estimation and Imaging of Complex Scenes

- Separation of Moving and Stationary Target Data

- Numerical Simulations

## Optimization Methods in Motion Estimation

## Summary and Future Work

# Summary

- ▶ Peaks (centroids) in phase-space of calibrated sub-apertures of the echoes correspond to motion of interest in data (target motion or platform perturbations). In progress: Coordinate information over multiple overlapping apertures.
- ▶ Wigner transform and ambiguity function give complementary information. Issues: Computational complexity. Tradeoffs between aperture size, resolution and SNR.
- ▶ Pre-processing of data to separate moving targets from stationary targets to decouple motion estimation and autofocus problems. The travel time based filtering seems to work best at present. Much more to do here.